

Investigation of the Nuclear Cross-Sections for Proton Capture Reactions in the Star Formation Process of the Galaxies

Rabab Muzhir J.^{1a*} and Al Najm M. N.^{1b}

¹*Department of Astronomy and Space, College of Science, University of Baghdad, Baghdad, Iraq*

^{a*} Corresponding author: rabab.mozher1107d@sc.uobaghdad.edu.iq

Abstract

This paper investigates the proton capture reactions ${}^7\text{Be}(p,\gamma){}^8\text{B}$, ${}^{12}\text{C}(p,\gamma){}^{13}\text{N}$, ${}^{14}\text{N}(p,\gamma){}^{15}\text{O}$, and ${}^{15}\text{N}(p,\gamma){}^{12}\text{C}$ in the proton-proton (p-p) chain and Carbon-Nitrogen-Oxygen cycle (CNO), which are essential for comprehending the development of main sequence stars in the initial stages of spiral and elliptical galaxy formation. This study investigates proton capture reactions in spiral and elliptical galaxies. The excitation functions were summarized, which describe the energy dependence of the nuclear reaction cross-sections, to analyze the (p, γ) interaction cross-sections of ${}^7\text{Be}(p,\gamma){}^8\text{B}$, ${}^{12}\text{C}(p,\gamma){}^{13}\text{N}$, ${}^{14}\text{N}(p,\gamma){}^{15}\text{O}$, and ${}^{15}\text{N}(p,\gamma){}^{12}\text{C}$, in the p-p series and CNO cycle with energy up to 8 MeV. In this work, the theoretical values from the ENDF/B-VII library were compared with the estimated database of proton capture cross-sections in hydrogen-burning stellar objects from CSC-GM and TALYS. Cross-sections can be calculated at low energies within the p-p chain and CNO cycle. Therefore, we were able to calculate the proton capture cross-sections of four of the investigated nuclear reactions, ${}^7\text{Be}(p,\gamma){}^8\text{B}$, ${}^{12}\text{C}(p,\gamma){}^{13}\text{N}$, ${}^{14}\text{N}(p,\gamma){}^{15}\text{O}$, and ${}^{15}\text{N}(p,\gamma){}^{12}\text{C}$, which are part of the p-p chain and CNO cycle in stellar nucleosynthesis in galaxies.

Article Info.

Keywords:

Cross Sections, p-p Chain, CNO Cycle, Spiral and Elliptical Galaxies, Star Formation.

Article history:

Received: Apr. 25, 2024

Revised: Aug. 03, 2024

Accepted: Aug. 17, 2024

Published: Dec 01, 2024

1. Introduction

Astronomical observations of the luminosity and chemical makeup of galaxies, stars, and supernova events, as well as the interstellar medium, provide evidence for nuclear processes [1-5]. How a particle is emitted during a nuclear reaction is essential for learning about the nucleus [6]. Nuclear reactions transpire as a result of the interaction between nuclei, protons, photons, and other particles. For example, in addition to photons and nucleons, protons (p), deuterium (d), tritium (t), neutrons (n), and the initial elements to be generated (H, He, Li, and Be), all interact with one another via nuclei [7-10]. Nuclear physics and astrophysics rely heavily on the neutron capture reaction [11]. All the atoms in the universe that are heavier than hydrogen and helium are made through nuclear reactions; this includes stars and nuclear reactors, both of which produce energy via nuclear processes [9]. Thermonuclear reaction rates in stars result in high-temperature differences, and these temperature variations further separate processes of the proton-proton (p-p) chain and the Carbon-Nitrogen-Oxygen (CNO) cycle, which are the two main hydrogen burning mechanisms in stars. Only a few interactions occur at insignificant rates at any stage of star evolution [12]. Primary processes create elements directly from nucleons and simple nuclei (like hydrogen and helium) in the same location where nucleosynthesis occurs. These processes are typical of the first generation of stars. Secondary processes depend on pre-existing elements produced by earlier stars. These pre-existing elements are incorporated into new stars and undergo further nucleosynthesis [13, 14].

Stars operate primarily through thermonuclear fusion reactions, which are primarily responsible for producing energy and creating the various nuclei inside the star. Proton-proton reaction chains and the CNO cycle, a group of nuclear reactions that convert hydrogen into helium, make burning hydrogen possible. For example, ${}^{14}\text{N}(p,\gamma){}^{15}\text{O}$ is considered the bottleneck of the first CNO cycle, and it controls the rate of its occurrence as well as the



star's arrival at the point where its brightness stops (its exit from the main sequence stage) and the burning of CNO in it.

The outward pressure from fusion reactions counteracts the internal gravitational pull in the first stage of hydrostatic combustion, maintaining the star's stability. A p-p chain enables hydrogen fusion. This process entails the amalgamation of hydrogen nuclei (protons) to generate helium while simultaneously discharging energy. The fusion process that is most prevalent in low-mass stars, such as the Sun, is known as the dominant fusion process. On the other hand, hydrogen burning in intermediate-mass stars and massive stars occurs through the CNO cycle. This method employs carbon, nitrogen, and oxygen as catalysts to transform hydrogen into helium. The CNO cycle has greater temperature dependence and efficiency in the higher core temperatures of these more massive stars [15].

In nuclear physics, star activity and the universe's observables are inextricably linked to nuclear structure. Understanding cross-sections (σ) for numerous types of nuclear reactions is crucial for interpreting astrophysical phenomena and developing the future of nuclear reactors [16, 17]. The cross-section represents the likelihood of a reaction occurring when two particles collide. The scattering cross-section is a quantitative measure of the frequency at which a specific interaction occurs between radiation and a target. More specifically, the cross-section is the rate of scattering as a function of the incoming radiation flux, which is calculated by dividing the number of particles that hit the target surface in a second by the surface area, assuming that the incoming radiation is composed of "particles," such as protons or neutrons. The number of energy levels per unit energy, or level density, is the number of energy levels per unit energy. This density level is a key factor that determines the cross-section of a nuclear reaction [18]. The standard units used to quantify cross-sections of nuclear reactions are barns (b). A scattering cross-section signifies an effective area whose size is proportional to the probability of interaction between the radiation and the target. Specifically, hydrogen burning occurs in intermediate-mass and massive stars via the CNO cycle [19, 20].

In the universe, the proportion of H and He is roughly 73% and 25% of the overall mass, respectively; C, N, and O are the most prevalent elements in the universe, following H and He [21]. The explanation of star existence relies on nuclear processes. The primary mechanism by which hydrogen undergoes combustion entails the fusion of four protons, forming a solitary ${}^4\text{He}$ nucleus. Hydrogen can undergo conversion into helium using two distinct reaction chains [22-26].

The cross-sections of specific proton capture reactions, known as "p-p fusion" give the Sun and other stars their energy. It occurs in the core of stars that are cooler than 15×10^6 °K and involves a reaction cycle that produces 25MeV of energy. The temperature at which a p-p cycle occurs is lower than that of the CNO cycle. Prominent bodies, including the Sun, divide the p-p chain into three discrete pathways called the ppI, ppII, and ppIII chains. The proton-proton fusion reaction ppI in stars, including the Sun, commences with the collision of two protons (p or ${}^1\text{H}$), which results in the formation of a heavy hydrogen atom ${}^2\text{H}$. During the second stage, the weak interaction between a ${}^2\text{H}$ nucleus and a proton produces a ${}^3\text{He}$ nucleus, releasing extremely energetic gamma rays. In the final stage, the fusion of two ${}^3\text{He}$ nuclei forms a stable ${}^4\text{He}$ nucleus. This process also releases two more protons ($2{}^1\text{H}$), which initiate the next round of the reaction. The Sun undergoes a continuous process in which it transforms around 655×10^6 tons of H into 650×10^6 tons of ${}^4\text{He}$ every second. When stars have masses greater than around $2 M_{\odot}$ and core temperatures greater than 18×10^6 °K, a unique chemical process known as the carbon-nitrogen cycle is the principal means of generating energy through the fusion of hydrogen into helium. The original situation is the final reaction of the ppI chain, but the later reaction could continue into the ppII or ppIII chains.

The CNO cycle is the primary mechanism for the stable burning of hydrogen in stars, occurring within a temperature range of 20×10^6 to 130×10^6 °K. The following sequence of processes elucidates the conversion of hydrogen into helium in this stellar cycle, specifically for stars exceeding the mass of the Sun. The CNO cycle includes successive steps: When the ^{12}C element absorbs a proton, it changes into ^{13}N and emits gamma rays. ^{13}N , an unstable isotope, undergoes radioactive decay and transforms into ^{13}C . The half-life of this decay process is around 10 minutes. The ^{13}C isotope undergoes proton capture, resulting in the emission of a gamma ray and the transformation into the ^{14}N isotope, which undergoes proton capture, resulting in the emission of a gamma ray and the transformation into ^{15}O . The ^{15}O isotope undergoes a β^+ decay and converts into ^{15}N . Ultimately, the ^{15}N isotope seizes a proton and then releases ^4He to complete the cycle and revert to ^{12}C [15, 25, 27-38].

The process by which two nuclei combine to form a compound nucleus is known as nuclear fusion. This is the basis for nucleosynthesis in stars. Reactions in the field of nuclear physics are frequently written as $A(a,b)B$ [39], where a is the projectile, A is the target nucleus, B represents the combination's relatively heavy nucleus, and b represents the lighter result. Specifically, a γ ray is the lighter result in a radiative capture. The capture reactions, whether (p,γ) or (α,γ) , make up a significant fraction of all nuclear events relevant to astrophysics. The Coulomb barrier is the electrical repulsion that two nuclei experience from each other's positive charges before they fuse. Most stellar scenarios occur at temperatures ranging from 10^7 to 10^9 K, starting at the Coulomb barrier threshold and going up to a few MeV [40]. The phenomenon known as quantum tunnelling, in which a particle's wave function may pass through potential barriers greater than its kinetic energy, is the origin of these processes [41, 42].

Penzias [43] Examining interstellar molecules has allowed the study of the galactic proportions of stable isotopes Si, C, N, O, S, and hydrogen. The results of this study indicated that there is a faster rate of star formation in the area of the galactic centre due to the increased amount of processed material, especially ^{13}C . Lalremruata et al. [44] used Talys-1.0, a nuclear simulation code with predefined general variables, to calculate excitation functions for the (n,p) reaction on 5 isotopes of nickel (^{58}Ni , ^{60}Ni , ^{61}Ni , ^{62}Ni , and ^{64}Ni).

Rosario et al. [45] study concluded that the potential of galaxies transitioning from active production of stars to inactivity is more likely to contain low- and moderate-luminosity active galactic nuclei (AGNs). They showed that AGNs are more frequently observed in starforming host galaxies. Pritychenko and Mughabghab [46] presented astronomical rates of reaction and neutron thermal cross sections for 843 reactants from the Evaluated Nuclear Data File (ENDF). Mason et al. [47] figured out how to group fifty galaxies into groups based on their shapes, ranging from late-type spiral galaxies (Sc, Sd, and Sm) to elliptical galaxies (E). Although most galaxies appear to contain an active galactic nucleus (AGN), the spectrum exhibits unique characteristics due to the sample AGN's luminosity. Ismail et al. [48] utilized the TALYS 1.6 code and gamma-ray incidence energies of up to 20 MeV and calculated the reaction cross-section of the $^{235}\text{U}(g,f)$ for multiple-level density simulations. Chemseddine et al. [49] predicted the chemical evolution of AGBn stars and understood their influence on the development of our galaxy (the Milk Way).

This article highlights a noteworthy display by the Laboratory for Underground Nuclear Astrophysics (LUNA), which significantly enhanced our understanding of the evolutionary mechanisms of AGB stars and the complexities associated with nuclear synthesis. LUNA has undertaken focused investigations into many reactions crucial for producing light components in the outer layer of hydrogen-burning material. The investigation of proton capture cross-sections on ^{17}O and ^{18}O has improved our understanding of the expected oxygen isotope ratios originating from AGB stars most CNO cycle activities, for which first data is now available.

2. Method of Calculating Cross-Section σ

Nuclear reaction rates are essential for investigating stars' energy generation and nucleosynthesis processes. Astrophysical reaction rates describing the change in the abundances due to nuclear reactions in an astrophysical environment are functions of the densities of the interacting nuclei, their relative velocities, and reaction cross-section [50, 51]. Nuclear physics 'role in understanding nucleosynthesis and stellar evolution involves measurements or computations of fundamental quantities, such as reaction cross-sections, nuclear masses, and β -decay rates. The various important capture reactions to understand the p-process nucleosynthesis are (n, γ) , (p, γ) , (α, γ) , etc. The present study focused on the proton capture (p, γ) reaction.

In the study of nuclear synthesis processes inside stars, nuclear reaction rates are one of its basic components, as they describe the change in the abundance of elements resulting from nuclear reactions inside stars [52, 53]. The role of nuclear physics is to contribute to understanding the evolution of stars by measuring or calculating the interactions cross-sections. For this reason, different capture reactions are important in understanding the p process, which is focused on in this work on the (p, γ) reactions within the p-p reaction chains and the CNO cycle. The cross-section of these reactions with the energy of the centre of mass of the reaction system $E < E_c$ is [54]

$$\sigma = S(E) \frac{1}{E} \exp(-2\pi \eta(E)) \quad (1)$$

where $S(E)$ is the scattering matrix of the reaction, and $\eta = \frac{Z_1 Z_2 e^2}{\hbar v}$ is the Sommerfeld parameter, Z_1 and Z_2 are the atomic numbers of the interacting nuclei, e is the elementary charge, \hbar is the reduced Planck's constant, and v is the relative velocity of the nuclei in the center-of-mass frame.

The ENDF library contains data on nuclear reactions for astrophysics, especially cross-sections of capture reactions, for example for stars AGB [55], suitable for understanding P-S processes. The proton capture cross-section rate is defined by the following formula [55]

$$\sigma(KT) = \frac{2}{\sqrt{\pi}} \frac{m_2^2}{(m_1+m_2)^2} \int_0^\infty \sigma(E_n) E_n \exp\left(-\frac{E_n m_2}{KT(m_1+m_2)}\right) dE_n \quad (2)$$

$$\sigma(KT) = \frac{2}{\sqrt{\pi}} \frac{m_2^2}{(m_1+m_2)^2} \int_0^\infty \sigma(E_n^L) E_n^L \exp\left(-\frac{E_n^L m_2}{KT(m_1+m_2)}\right) dE_n^L \quad (3)$$

where K and T are Boltzmann constant and the temperature of the system, respectively, E is the relative kinetic energy of the proton relative to the target, E_n^L is the laboratory energy of the system, and m_1, m_2 are the masses of the proton and the target, respectively.

The total cross-section gives the proton capture reaction according to the Glanber Model

$$\sigma = \int \frac{d\mathbf{q}^{\rightarrow}}{k^2} |F(\mathbf{q}^{\rightarrow})|^2 \tau \quad (4)$$

where $F(\mathbf{q}^{\rightarrow})$ is the scattering capacity for such a reaction within the Glanber Model, which is given in the form [54, 56]:

$$F(q \rightarrow) = \frac{ik}{2\pi} \int db e^{i q \cdot b \rightarrow} \langle \Psi_a \Theta_e | 1 - \prod_{i \in P} \prod_{j \in \tau} (1 - F_{ij}) | \Psi_0 \Theta_0 \rangle \quad (5)$$

where τ is the target core, P is the projectile core, k is the momentum of the projectile, Ψ_0 is the intrinsic wave function of the projectile, Ψ_a is the wave function in the (a) plane, Θ_0 and Θ_e are the eigenvector functions of the target and the (a) plane, b is the impact factor between the projectile and the target, and q is the transferred momentum.

3. Results and Discussion

The work focused on analyzing the cross-sections of the (p,γ) reactions for ${}^7\text{Be}(p,\gamma){}^8\text{B}$, ${}^2\text{C}(p,\gamma){}^{13}\text{N}$, ${}^{14}\text{N}(p,\gamma){}^{15}\text{O}$, and ${}^{13}\text{C}(p,\gamma){}^{14}\text{N}$ in the p-p chain and CNO cycle. The study used two programs and compared their results with the available experimental data in the ENDF/B-VII library [3, 57, 58]. The estimated values for nuclear fusion cross-sections in hydrogen-burning stellar objects were compared with the theoretical data obtained from the ENDF/B-VII library [49,50] of spiral and elliptical galaxies [59]. The initial contact was ${}^7\text{Be}(p,\gamma){}^8\text{B}$, followed by ${}^{12}\text{C}(p,\gamma){}^{13}\text{N}$ for spiral galaxies, ${}^{14}\text{N}(p,\gamma){}^{15}\text{O}$, and ${}^{13}\text{C}(p,\gamma){}^{14}\text{N}$ for elliptical galaxies. The TALYS computer coding system can simulate nuclear reactions and calculate cross-sections across a wide energy range, from 1 keV to 1 GeV, making it a valuable tool for studying various nuclear processes in astrophysics and nuclear physics [57].

The calculation results of the theoretical cross-section values using the CSC-GM and TALYS models are presented in Figs. 1-4 with data from the ENDF/B-VII library. The first and second forms for spiral galaxies were used. Fig. 1 shows the reaction cross-sections for ${}^7\text{Be}(p,\gamma){}^8\text{B}$ in a ppIII chain between 0 and 8 MeV based on simple calculations. The star generation rate is extremely high in both the CSC-GM and ENDF systems. While in the TALYS system, the cross-section of the star formation rate is less steep than in the two cases mentioned above. Despite the increase in values, TALYS restricted the reaction cross-section value to approximately 5 MeV energy. Simultaneously, the CSC-GM computer, TALYS code, and ENDF systems demonstrated a rise in the energy range between 6.5 MeV and 8 MeV.

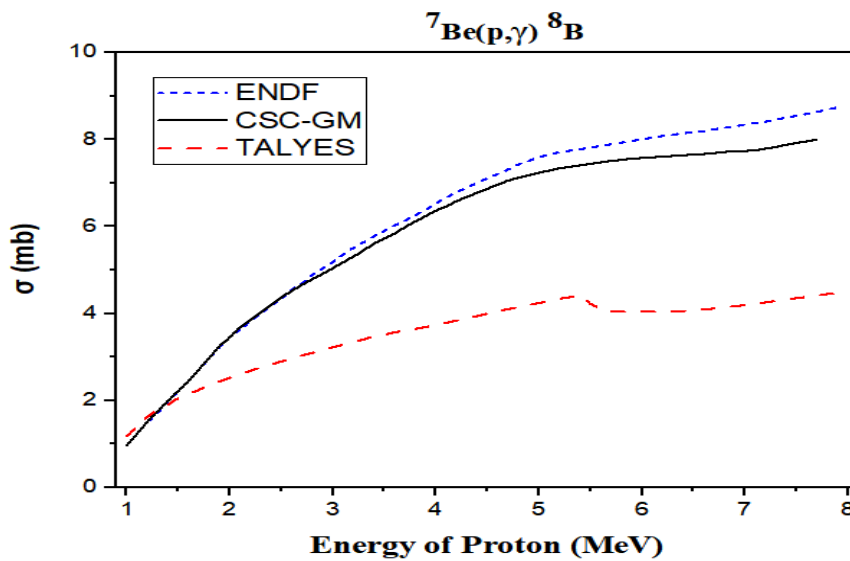


Figure 1: A theoretical cross-section estimate for the ${}^7\text{Be}(p,\gamma){}^8\text{B}$ reaction at 8 MeV for a spiral galaxy.

Fig. 2 shows the $^{12}\text{C}(p,\gamma)^{13}\text{N}$ reaction cross-section accumulating in the CNO cycle. This figure illustrates how the theoretical results from TALYS and ENDF agree well and how the data closely matches ENDF at about 4 MeV. This signifies the continuation of the fusion process. The second characteristic of CSC-GM is that it does not begin at a particular value of cross-section, whereas ENDF and TALYS begin above 0.001mb and near 0.004 mb, respectively. This is due to the proportion of components that undergo fusion. The likelihood of the reaction occurring inside one program varies, and the best program that emerged is the CSC-GM since starting from 0 means that the fusion process began at zero. The procedure continued and produced the most significant probability of 0.008 mb. This suggests that spiral galaxies have very young stars rich in gaseous and stellar material, which reflects a high level of nuclear fusion activity in young stars.

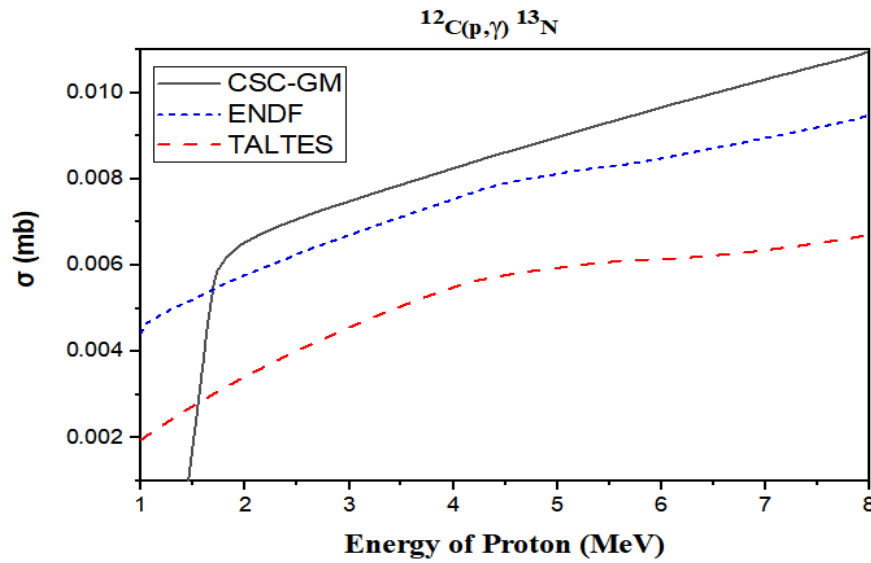


Figure 2: The theoretical cross-sections for the $^{12}\text{C}(p,\gamma)^{13}\text{N}$ reaction at 8 MeV for a spiral galaxies.

For elliptical galaxies in the CNO cycle, the third and fourth reaction cross-section estimates are $^{15}\text{N}(p,\alpha)^{12}\text{C}$, and this reaction involves a p interacting with a ^{15}N nucleus. The proton is absorbed, and an alpha particle (α) is emitted, resulting in the formation of a ^{12}C nucleus, as shown in Eq. (6)



$^{13}\text{C}(p,\gamma)^{14}\text{N}$ reaction involves a proton (p) interacting with a ^{13}C nucleus. The proton is absorbed, and γ is emitted, resulting in the formation of ^{14}N nucleus, as shown in Eq.(7)



The Fig. 3 demonstrates a strong correlation between the cross-section and the proton energy, reaching 800 eV. All cross-section measurements indicate an increasing trend up to roughly 7 MeV but have stable and consistent values after 7 MeV, indicating very high temperatures. This is because the heavy element in the nuclear fusion process and the likelihood of the reaction happening rise dramatically, and this rise is thought to be extremely quick. This relationship between star creation and occurrence indicates that elliptical galaxies have older stars and poorer star formation.

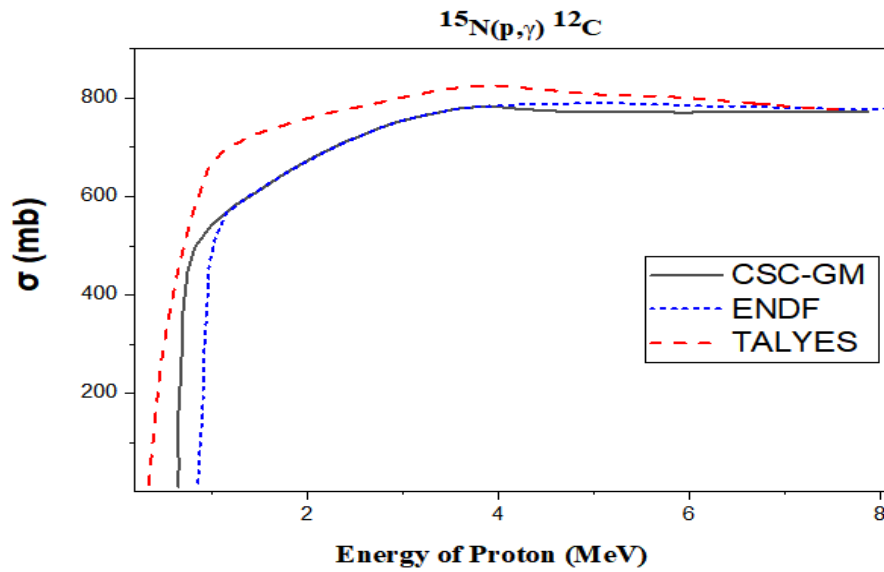


Figure 3: The theoretical cross-sections for the $^{15}\text{N}(p, \gamma)^{12}\text{C}$ reaction at 8 MeV for elliptical galaxies.

The $^{13}\text{C}(p, g)^{14}\text{N}$ reaction studied is the fourth reaction in the elliptical galaxies and the last $^{12}\text{C}(p, \gamma)^{13}\text{N}$ reaction in the CNO cycle. The difference in the cross-section calculations performed by each computer program can be observed. The discordance between the CSC-GM, TALYS, and the ENDF computer data up to 2.5 MeV was noted, and there was a good agreement at 2.5 MeV. Also, as the line from CSC-GM decreased to 2.5 MeV, the line from TALYS increased. The literature has no experimental data for the $^{12}\text{C}(p, \gamma)^{13}\text{N}$ (See Fig. 4). The $^{13}\text{C}(p, \gamma)^{14}\text{N}$ is a direct capture ($Q= 7.55$. MeV) interaction that is dominated by the E1 transition from the incoming s-d wave to the bonnal wave of three states and the next four excited states in ^{14}N . This interaction exhibits astrophysical behavior in the stars, mainly in the CNO cycle. The difference in cross-sections for the three models can be noted because the abundance of ^{13}C changes in the stellar medium to have ^{14}N as the heaviest stable odd-odd nucleus. Fig. 4 shows that the cross-section of this capture interaction showed a strong peak for α calculations by the CSC-GM and ENDF energy $E_p \approx 1$ MeV, while a large difference in cross-section in TALYES. A fair agreement of the results is shown in $E_p \approx 3$ MeV for the ENDF and TALYES.

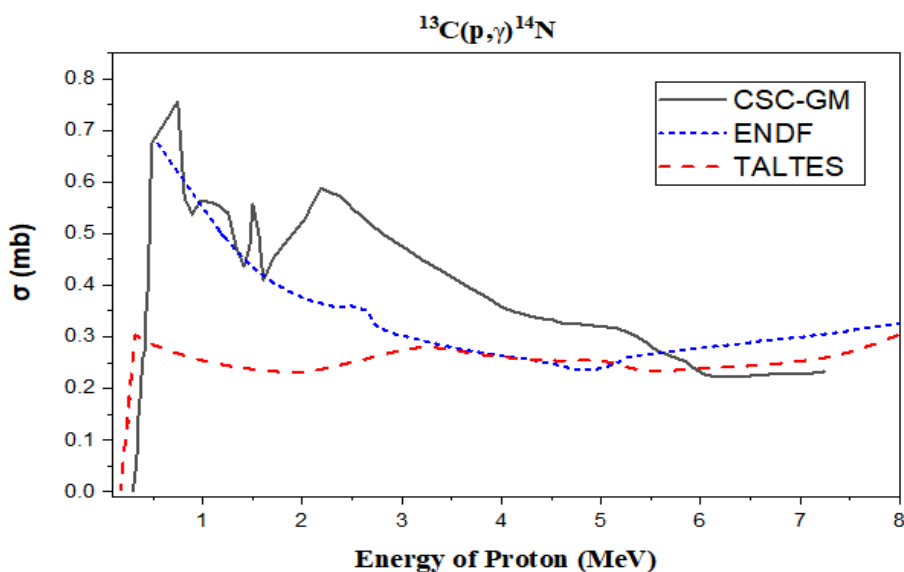


Figure 4: The theoretical cross sections of the $^{13}\text{C}(p, \gamma)^{14}\text{N}$ reaction at 8 MeV for an elliptical galaxy.

4. Conclusions

A key component of our knowledge of the evolution of galaxies is the cross-section of star formation in their core regions. Given that they represent a major portion of the ongoing star formation in nearby galaxies and contain significant quantities of hydrogen and helium gases, rings of star-forming nuclei are important characteristics in this perspective. In this study, the star formation rates in spiral and elliptical galaxies were analyzed using the proton capture of the star formation cross-section in these systems. In the present article, the cross-section of the (p, γ) interactions for ^7Be , ^{12}C , ^{13}C , and ^{15}N nuclei within the p-p chain and CNO cycle in stars were computed in the energy range from (0–8) MeV using TALYS 1.6 and CSC-GM computer codes. For these nuclei, cross-sections can be calculated at low energies within the p-p chain and CNO cycle. The results in CSC-GM showed that spiral galaxies have high star formation rates because the interaction cross-sections for $^7\text{Be}(p,\gamma)^8\text{B}$ in a p-p chain increase to 8 MeV. Our findings indicated a significant variation in the cross-section in TALYES, but a prominent peak for α estimated by CSC-GM and ENDF, at energy $E_p \approx 1$ MeV in the proton capture interaction cross-section. TALYES and ENDF agreed quite well with the $E_p \approx 3$ MeV values. Interaction cross-section estimates were performed for elliptical galaxies in the CNO cycle. The results showed that elliptical galaxies have older stars and less star formation. As a result, spiral galaxies have plenty of gas (such as H and He) and dust molecules responsible for star formation. In contrast, elliptical galaxies appeared to have exhausted all their energy sources, leaving relatively little energy available for the birth of young stars.

Acknowledgments

The authors thank the personal support provided by Assist. Prof. Dr. Akram Mohammed Ali from the Department of Physics, College of Science, Anbar University.

Conflict of interest

Authors declare that they have no conflict of interest.

References

1. M. N. Al Najm, H. H. Al-Dahlaki, and B. A. Alkotbe, *Iraqi J. Sci.* **64**, 6620 (2023). DOI: 10.24996/ijs.2023.64.12.41.
2. M. Al Najm, Y. Rashed, and H. Al-Dahlaki, *Baghdad Sci. J.* **21**, 1 (2024). DOI: 10.21123/bsj.2024.10452.
3. M. M. Zamal and M. N. Al Najm, *Iraqi J. Sci.* **64**, 3176 (2023). DOI: 10.24996/ijs.2023.64.6.44.
4. A. Silvestri and M. Trodden, *Rep. Prog. Phys.* **72**, 096901 (2009). DOI: 10.1088/0034-4885/72/9/096901.
5. S. Goriely, S. Hilaire, and A. J. Koning, *Astro. Astrophys.* **487**, 767 (2008). DOI: 10.1051/0004-6361:20078825.
6. S. S. Shaker, F. G. Naima, and A. M. Ali, *American J. Phys. Applic.* **2**, 52 (2014). DOI: 10.11648/j.ajpa.20140202.12.
7. A. A. Khlil Maroof, A. M. Ali, and S. S. Shafik, *IOP Conf. Ser. Mat. Sci. Eng.* **928**, 072145 (2020). DOI: 10.1088/1757-899X/928/7/072145.
8. M. H. Jasim, *Iraqi J. Sci.* **57**, 1964 (2023).
9. C. A. Bertulani, *Encyclopedia of Applied Physics* (Online, Wiley-VCH Verlag GmbH & Co. KGaA (Ed.), 2014), p.45.
10. R. Karki, *Himal. Phys.* **1**, 79 (2011). DOI: 10.3126/hj.v1i0.5186.
11. L. T. Ali and A. A. Selman, *Iraqi J. Sci.* **62**, (2021). DOI: 10.24996/10.24996/ijs.2021.62.5.36.
12. J. N. Bahcall, M. H. Pinsonneault, and S. Basu, *Astrophys. J.* **555**, 990 (2001). DOI: 10.1086/321493.
13. D. Watson, C. J. Hansen, J. Selsing, A. Koch, D. B. Malesani, A. C. Andersen, J. P. U. Fynbo, A. Arcones, A. Bauswein, S. Covino, A. Grado, K. E. Heintz, L. Hunt, C. Kouveliotou, G. Leloudas, A. J. Levan, P. Mazzali, and E. Pian, *Nature* **574**, 497 (2019). DOI: 10.1038/s41586-019-1676-3.
14. W. R. Hix and F.-K. Thielemann, *J. Comput. Appl. Math.* **109**, 321 (1999). DOI: 10.1016/S0377-0427(99)00163-6.
15. E. G. Adelberger, A. García, R. G. H. Robertson, K. A. Snover, A. B. Balantekin, K. Heeger, M. J. Ramsey-Musolf, D. Bemmerer, A. Junghans, C. A. Bertulani, J. W. Chen, H. Costantini, P. Prati, M. Couder, E. Uberseder, M. Wiescher, R. Cyburt, B. Davids, S. J. Freedman, M. Gai, D. Gazit, L. Gialanella,

- G. Imbriani, U. Greife, M. Hass, W. C. Haxton, T. Itahashi, K. Kubodera, K. Langanke, D. Leitner, M. Leitner, P. Vetter, L. Winslow, L. E. Marcucci, T. Motobayashi, A. Mukhamedzhanov, R. E. Tribble, K. M. Nollett, F. M. Nunes, T. S. Park, P. D. Parker, R. Schiavilla, E. C. Simpson, C. Spitaleri, F. Strieder, H. P. Trautvetter, K. Suemmerer, and S. Typel, *Rev. Mod. Phys.* **83**, 195 (2011). DOI: 10.1103/RevModPhys.83.195.
16. A. A. Aziz, N. S. Ahmad, S. Ahn, W. Aoki, M. Bhuyan, K.-J. Chen, G. Guo, K. I. Hahn, T. Kajino, H. A. Kassim, D. Kim, S. Kubono, M. Kusakabe, A. Li, H. Li, Z. H. Li, W. P. Liu, Z. W. Liu, T. Motobayashi, K.-C. Pan, T. S. Park, J.-R. Shi, X. Tang, W. Wang, L. Wen, M.-R. Wu, H.-L. Yan, and N. Yusof, *AAPPS Bulletin* **31**, 18 (2021). DOI: 10.1007/s43673-021-00018-z.
 17. A. P. D. Ramirez, Ph.D Thesis, Ohio University, 2014.
 18. J. F. Mohammad, A. D. Salloum, and H. A. Al-Jabbar, *Iraqi J. Sci.* **63**, 1977 (2022). DOI: 10.24996/ij.s.2022.63.5.12.
 19. G. Lorusso, S. Nishimura, Z. Y. Xu, A. Jungclaus, Y. Shimizu, G. S. Simpson, P. A. Söderström, H. Watanabe, F. Browne, P. Doornenbal, G. Gey, H. S. Jung, B. Meyer, T. Sumikama, J. Taprogge, Z. Vajta, J. Wu, H. Baba, G. Benzoni, K. Y. Chae, F. C. L. Crespi, N. Fukuda, R. Gernhäuser, N. Inabe, T. Isobe, T. Kajino, D. Kameda, G. D. Kim, Y. K. Kim, I. Kojouharov, F. G. Kondev, T. Kubo, N. Kurz, Y. K. Kwon, G. J. Lane, Z. Li, A. Montaner-Pizá, K. Moschner, F. Naqvi, M. Niikura, H. Nishibata, A. Odahara, R. Orlandi, Z. Patel, Z. Podolyák, H. Sakurai, H. Schaffner, P. Schury, S. Shibagaki, K. Steiger, H. Suzuki, H. Takeda, A. Wendt, A. Yagi, and K. Yoshinaga, *Phys. Rev. Lett.* **114**, 192501 (2015). DOI: 10.1103/PhysRevLett.114.192501.
 20. R. J. Ascutto and J. S. Vaagen, *Europ. Phys. J. H* **49**, 3 (2024). DOI: 10.1140/epjh/s13129-023-00060-5.
 21. G. C. Dehne, *Term. Int. J. Theor. Appl. Iss. Speci. Commun.* **4**, 347 (1997). DOI: 10.1075/term.4.2.08deh.
 22. N. Przybilla, M. Firnstein, M. F. Nieva, G. Meynet, and A. J. A. Maeder, *Astro. Astrophys.* **517**, A38 (2010). DOI: 10.1051/0004-6361/201014164.
 23. A. M. Ali and H. M. Mohammed, *Iraqi J. Sci.* **63**, 2514 (2022). DOI: 10.24996/ij.s.2022.63.6.18.
 24. F. Hoyle, *Astrophys. J. Suppl.* **1**, 121 (1954). DOI: 10.1086/190005.
 25. H. A. Bethe, *Phys. Rev.* **55**, 434 (1939). DOI: 10.1103/PhysRev.55.434.
 26. A. A. Selman and H. S. Jasim, *J. Appl. Phys.* **8**, 43 (2016). DOI: 10.9790/4861-0804014352
 27. R. K. Wallace and S. E. Woosley, *Astrophys. J. Suppl. Ser.* **45**, 389 (1981). DOI: 10.1086/190717.
 28. A. M. Ali, *Int. J. Mod. Phys. E* **31**, 2250041 (2022). DOI: 10.1142/s0218301322500410.
 29. B. W. Carroll and D. A. Ostlie, *An Introduction to Modern Astrophysics* (Cambridge, England, Cambridge University Press, 2017).
 30. R. J. Deboer, J. Görres, M. Wiescher, R. E. Azuma, A. Best, C. R. Brune, C. E. Fields, S. Jones, M. Pignatari, D. Sayre, K. Smith, F. X. Timmes, and E. Uberseder, *Rev. Mod. Phys.* **89**, 035007 (2017). DOI: 10.1103/RevModPhys.89.035007.
 31. E. G. Adelberger, S. M. Austin, J. N. Bahcall, A. B. Balantekin, G. Bogaert, L. S. Brown, L. Buchmann, F. E. Cecil, A. E. Champagne, L. De Braekeleer, C. A. Duba, S. R. Elliott, S. J. Freedman, M. Gai, G. Goldring, C. R. Gould, A. Gruzinov, W. C. Haxton, K. M. Heeger, E. Henley, C. W. Johnson, M. Kamionkowski, R. W. Kavanagh, S. E. Koonin, K. Kubodera, K. Langanke, T. Motobayashi, V. Pandharipande, P. Parker, R. G. H. Robertson, C. Rolfs, R. F. Sawyer, N. Shaviv, T. D. Shoppa, K. A. Snover, E. Swanson, R. E. Tribble, S. Turck-Chièze, and J. F. Wilkerson, *Rev. Mod. Phys.* **70**, 1265 (1998). DOI: 10.1103/RevModPhys.70.1265.
 32. R. Kunz, M. Jaeger, A. Mayer, J. W. Hammer, G. Staudt, S. Harissopulos, and T. Paradellis, *Phys. Rev. Lett.* **86**, 3244 (2001). DOI: 10.1103/PhysRevLett.86.3244.
 33. C. R. Brune, J. Daly, R. Detwiler, B. Fisher, W. H. Geist, J. Görres, H. J. Karwowski, R. W. Kavanagh, D. S. Leonard, P. Tischhauser, K. D. Veal, and M. Wiescher, *Nucl. Phys. A* **688**, 263 (2001). DOI: 10.1016/S0375-9474(01)00711-4.
 34. L. Buchmann, P. Tischhauser, R. E. Azuma, R. Detwiler, U. Giesen, J. Görres, M. Heil, J. Hinnefeld, F. Käppeler, J. J. Kolata, H. Schatz, A. Shotton, E. Stech, S. Vouzoukas, and M. Wiescher, *Nucl. Phys. A* **688**, 259 (2001). DOI: 10.1016/S0375-9474(01)00710-2.
 35. J. Görres, C. Arlandini, U. Giesen, M. Heil, F. Käppeler, H. Leiste, E. Stech, and M. Wiescher, *Phys. Rev. C* **62**, 055801 (2000). DOI: 10.1103/PhysRevC.62.055801.
 36. T. Rauscher, F. K. Thielemann, J. Görres, and M. Wiescher, *Nucl. Phys. A* **675**, 695 (2000). DOI: 10.1016/S0375-9474(00)00182-2.
 37. H. A. Bethe and C. L. Critchfield, *Physical Review* **54**, 248 (1938). DOI: 10.1103/PhysRev.54.248.
 38. E. E. Salpeter, *Astrophys. J.* **116**, 649 (1952). DOI: 10.1086/145656.
 39. C. L. Jiang, B. B. Back, H. Esbensen, R. V. F. Janssens, K. E. Rehm, and X. D. Tang, *J. Phys. Conf. Ser.* **312**, 042011 (2011). DOI: 10.1088/1742-6596/312/4/042011.
 40. M. H. Jasim and M. T. Idrees, *Iraqi J. Sci.* **57**, 910 (2022).
 41. L. T. Ali and A. A. Selman, *J. Phys. Conf. Ser.* **1818**, 012110 (2021). DOI: 10.1088/1742-6596/1818/1/012110.
 42. G. Gamow, *Zeitsch. Phys.* **51**, 204 (1928). DOI: 10.1007/BF01343196.

43. A. A. Penzias, Science **208**, 663 (1980). DOI: 10.1126/science.208.4445.663.
44. B. Lalremruata, S. Ganesan, V. N. Bhoraskar, and S. D. Dhole, Ann. Nucl. Ener. **36**, 458 (2009). DOI: 10.1016/j.anucene.2008.11.030.
45. D. J. Rosario, P. Santini, D. Lutz, H. Netzer, F. E. Bauer, S. Berta, B. Magnelli, P. Popesso, D. M. Alexander, W. N. Brandt, R. Genzel, R. Maiolino, J. R. Mullaney, R. Nordon, A. Saintonge, L. Tacconi, and S. Wuyts, Astrophys. J. **771**, 63 (2013). DOI: 10.1088/0004-637X/771/1/63.
46. B. Pritychenko and S. F. Mughabghab, Nucl. D. Sheets **113**, 3120 (2012). DOI: 10.1016/j.nds.2012.11.007.
47. R. E. Mason, A. Rodríguez-Ardila, L. Martins, R. Riffel, O. G. Martín, C. R. Almeida, D. R. Dutra, L. C. Ho, K. Thanjavur, H. Flohic, A. Alonso-Herrero, P. Lira, R. Mcdermid, R. A. Riffel, R. P. Schiavon, C. Winge, M. D. Hoenig, and E. Perlman, Astrophys. J. Suppl. Ser. **217**, 13 (2015). DOI: 10.1088/0067-0049/217/1/13.
48. I. H. Sarpün, A. Aydın, and H. Pekdoğan, EPJ Web Conf. **146**, 05015 (2017). DOI: 10.1051/epjconf/201714605015.
49. C. Ananna, F. Barile, A. Boeltzig, C. G. Bruno, F. Cavanna, G. F. Ciani, A. Compagnucci, L. Csedreki, R. Depalo, F. Ferraro, E. Masha, D. Piatti, D. Rapagnani, and J. Skowronski, Universe **8**, 4 (2022). DOI: 10.3390/universe8010004.
50. K. Langanke and M. Wiescher, Rep. Prog. Phys. **64**, 1657 (2001). DOI: 10.1088/0034-4885/64/12/202.
51. C. Iliadis, *Nuclear Physics of Stars* (Chapel Hill, US, John Wiley & Sons, 2015).
52. T. Rauscher, N. Dauphas, I. Dillmann, C. Fröhlich, Z. Fülöp, and G. Gyürky, Rep. Prog. Phys. **76**, 066201 (2013). DOI: 10.1088/0034-4885/76/6/066201.
53. W. A. Fowler, G. R. Caughlan, and B. A. Zimmerman, Ann. Rev. Astro. Astrophys. **5**, 525 (1967). DOI: 10.1146/annurev.aa.05.090167.002521.
54. I. Ray and A. Deb, Chinese Phys. C **48**, 064001 (2024). DOI: 10.1088/1674-1137/ad2dc3.
55. M. Busso, R. Gallino, and G. J. Wasserburg, Ann. Rev. Astro. Astrophys. **37**, 239 (1999). DOI: 10.1146/annurev.astro.37.1.239.
56. C. Elster, T. Lin, W. Glöckle, and S. Jeschonnek, Phys. Rev. C **78**, 034002 (2008). DOI: 10.1103/PhysRevC.78.034002.
57. A. Koning, S. Hilaire, and S. Goriely, *Talys-1.6 a Nuclear Reaction Program, User Manual* (Wien, Wien, Österreich, Arjan Koning, 2013).
58. S. Küküksucu, M. Yiğit, and N. Paar, Universe **8**, 25 (2022). DOI: 10.3390/universe8010025.
59. M. J. Rabab and M. N. Al Najm, Iraqi J. Sci. **65**, 1762 (2024). DOI: 10.24996/ij.s.2024.65.3.45.

دراسة المقاطع العرضية النووية لتفاعلات التقاط البروتون في عملية تكوين النجوم في المجرات

رباب مزهر جاسم¹ ومحمد ناجي ال نجم¹
 تقسم الفلك والفضاء، كلية العلوم، جامعة بغداد، بغداد، العراق

الخلاصة

تبحث هذه الورقة في تفاعلات التقاط البروتون ${}^7\text{Be}(p,\gamma){}^8\text{B}$, ${}^{12}\text{C}(p,\gamma){}^{13}\text{N}$, ${}^{14}\text{N}(p,\gamma){}^{15}\text{O}$, ${}^{15}\text{N}(p,\gamma){}^{12}\text{C}$ و دورة الكربون-النيتروجين-الأكسجين (CNO)، والتي تعد ضرورية لفهم تطور نجوم التسلسل الرئيسي في المراحل الأولية من تكوين المجرات الحلزونية والإهليلجية. هذه الدراسة تستقصي في تفاعلات التقاط البروتون في المجرات الحلزونية والإهليلجية. باستخدام OriginPro، قمنا بتلخيص وظائف الإثارة لتحليل المقاطع العرضية للتفاعلات (p,γ) لـ ${}^7\text{Be}(p,\gamma){}^8\text{B}$ و ${}^{12}\text{C}(p,\gamma){}^{13}\text{N}$ و ${}^{14}\text{N}(p,\gamma){}^{15}\text{O}$ و ${}^{15}\text{N}(p,\gamma){}^{12}\text{C}$ في سلسلة p-p ودورة CNO بطاقة تصل إلى حوالي 8 ميكا إلكترون فولت. في هذا العمل، قمنا بمقارنة القيم النظرية من مكتبة ENDF/B-VII مع قاعدة البيانات المقطرة لمقاطع التقاط البروتون في الأجرام النجمية التي تحرق الهيدروجين من CSC-GM و TALYS. تم حساب المقاطع العرضية عند الطاقات المنخفضة داخل سلسلة pp ودورة CNO. لذلك، تمكنا من حساب التفاعلات النووية الأربعة التي تم التحقيق فيها فقط وهي ${}^7\text{Be}(p,\gamma){}^8\text{B}$, ${}^{12}\text{C}(p,\gamma){}^{13}\text{N}$, ${}^{14}\text{N}(p,\gamma){}^{15}\text{O}$, ${}^{15}\text{N}(p,\gamma){}^{12}\text{C}$ ، والتي تعد جزءًا من سلسلة p-p ودورة CNO التخليق النووي النجمي في المجرات.

الكلمات المفتاحية: المقاطع العرضية، سلسلة p-p، دورة CNO، المجرات الحلزونية والإهليلجية، النشوء النجمي.